Bioorganic & Medicinal Chemistry 19 (2011) 5639–5647

Contents lists available at ScienceDirect

Bioorganic & Medicinal Chemistry

journal homepage: www.elsevier.com/locate/bmc

A novel 3-arylethynyl-substituted pyrido[2,3,-*b*]pyrazine derivatives and pharmacophore model as Wnt2/β-catenin pathway inhibitors in non-small-cell lung cancer cell lines

Young-Dae Gong [a,*,†], Mi-Sook Dong [b,*,†], Sang-Bum Lee [b], Nayeon Kim [a], Mi-Seon Bae [a], Nam-Sook Kang [c]

[a] Center for Innovative Drug Library Research, Dongguk University, Pil-dong 3-ga, Jung-gu, Seoul 100-715, Republic of Korea
[b] Graduate School of Biotechnology, Korea University, Seoul 136-701, Republic of Korea
[c] Center for Drug Discovery Platform Technology, Korea Research Institute of Chemical Technology, PO Box 107, Singseongno, Yuseong-gu, Daejeon 305-600, Republic of Korea

ARTICLE INFO

Article history:
Received 11 May 2011
Revised 14 July 2011
Accepted 15 July 2011
Available online 23 July 2011

Keywords:
Wnt2
β-Catenin
Pyrido[2,3,-*b*]pyrazines
Inhibitors
Anti-cancer
Pharmacophore

ABSTRACT

We developed Wnt/β-catenin inhibitors by identifying 13 number of 3-arylethynyl-substituted pyrido[2,3,-*b*]pyrazine derivatives that were able to inhibit the Wnt/β-catenin signal pathway and cancer cell proliferation. In the optimization process, a series of 2,3,6-trisubstituted pyrido[2,3,-*b*]pyrazine core skeletons showed were shown to higher activity than 2,3,6-trisubstituted quinoxaline's and thus hold promise for use as potential small-molecule inhibitors of the Wnt/β-catenin signal pathway in non-small-cell lung cancer cell (NSCLC) lines. And we have studied the pharmacophore mapping for compound **954**, which presented the highest activity with a fit value of 2.81. The pharmacophore mapping for the compounds including **954**, pyrido[2,3,-*b*]pyrazine core had hydrogen-bond acceptor site and hydrophobic center roles.

1. Introduction

Wnt signaling is one of the key signaling pathways that regulate cell proliferation, differentiation, and morphogenesis.[1,2] Wnt proteins constitute a family of highly conserved secreted glycoproteins that play multiple roles in the development and progression of diseases. Aberrant activation of the canonical Wnt signaling pathway is related to many human cancers, including colon carcinoma and melanoma.[3,4] β-Catenin is an essential component of cell to cell interaction and in the Wnt signal pathway plays an important role as a transcriptional activator with T-cell factor (TCF)/lymphoid enhancer factor (LEF). In the absence of Wnt protein, the level of cytosolic β-catenin is maintained low through the degradation of β-catenin by machinery of destruction complex. Activation of Wnt signaling inhibits GSK3β activity and accumulates cytosolic β-catenin level. The elevated level of β-catenin leads to translocation β-catenin in the nucleus and subsequently the complex formation with TCF/LEF that induces target gene expression, such as cyclin D1, c-Myc and survivin.

Lung cancer is the leading cause of cancer-related mortality worldwide. Studies have shown that APC or β-catenin mutations lead to the accumulation of nuclear β-catenin, which is associated with greater than 80% of familial colorectal cancers. However, these mutations are found rarely in lung cancers. Although extensive research on the Wnt pathway and cancer has been performed in colon tumors, more recent work has demonstrated that the Wnt pathway may play a significant role in lung cancer.[5]

The mRNA of human Wnt2 is highly expressed in fetal lung and weakly expressed in the placenta.[6] Inappropriate activation of the Wnt2/β-catenin pathway has been reported in many human cancers, including colorectal, gastric, breast, and cervical cancers.[7–9] You[10] demonstrated that the Wnt2 protein was overexpressed in freshly resected human NSCLC tissues and that inhibition of Wnt2-mediated signaling by siRNA or a monoclonal antibody induced programmed cell death in the NSCLC line A549. Moreover, the anti-Wnt2 antibody was shown to inhibit cell growth of primary cultures obtained from patients suffering from NSCLC. The importance of Wnt2 in the mediation of normal and pathological processes has motivated considerable efforts to identify β-catenin inhibitors. Although a wealth of inhibitory compounds is available, the generation of β-catenin inhibitors with selectivity toward individual Wnt isoforms has proven to be challenging. In particular, good drug-like small organic molecule for Wnt inhibitors are rare[11] though several small molecules were reported as hit or lead

* Corresponding authors. Tel.: +82 2 2260 3206; fax: +82 2 2290 1349 (Y.-D.G.); tel.: +82 2 3290 4146; fax: +82 2 3290 3951 (M.-S.D.).
E-mail addresses: ydgong@dongguk.edu (Y.-D. Gong), msdong@korea.ac.kr (M.-S. Dong).
† Co-corresponding authors were same contributed for this paper.

0968-0896/$ - see front matter © 2011 Elsevier Ltd. All rights reserved.
doi:10.1016/j.bmc.2011.07.028

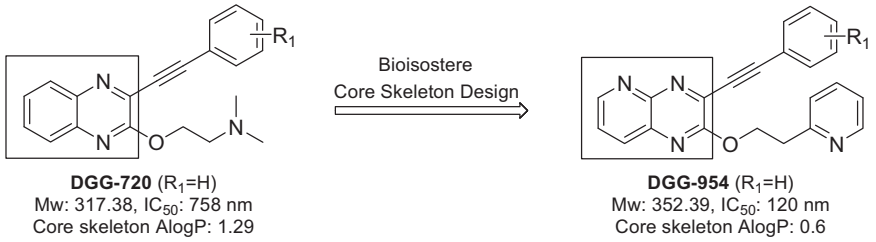

Figure 1. Optimization and design strategies for the Wnt2/β-catenin pathway inhibitors of the pyrido[2,3,-*b*]pyrazine core skeleton based on the bioisostere concept from the previous quinoxaline hit compound.

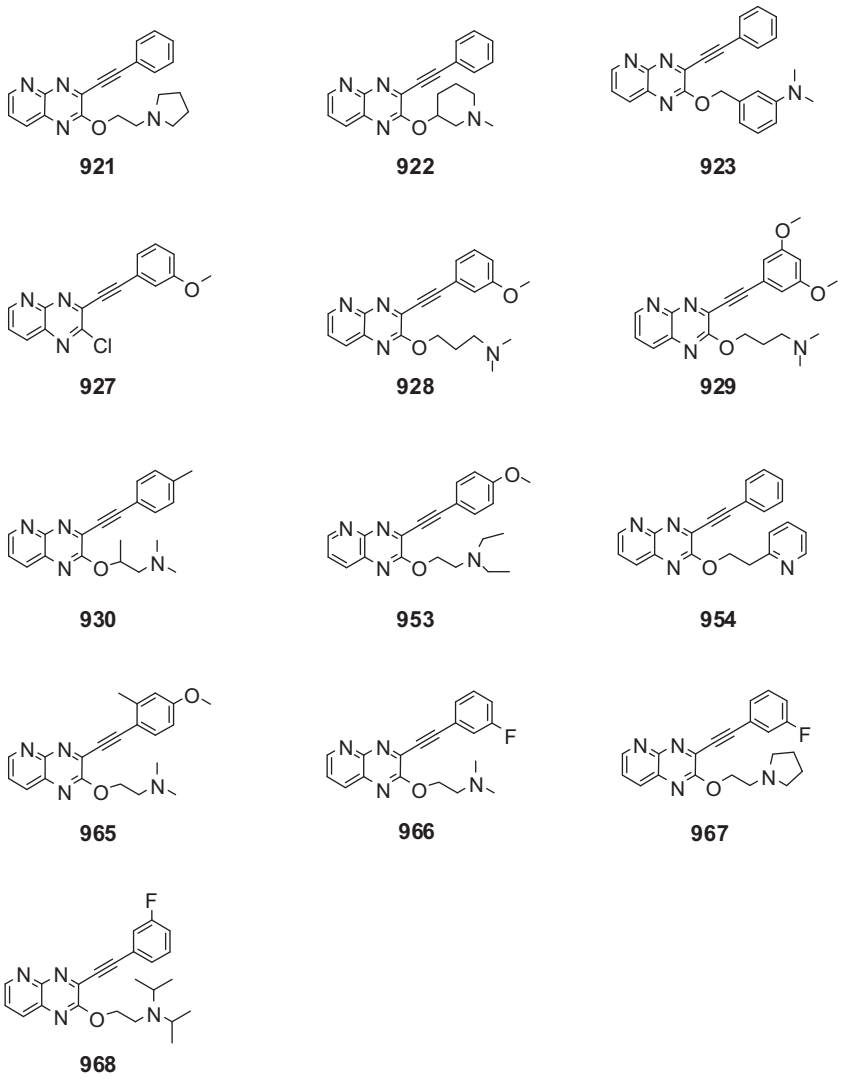

Figure 2. Structure of the Wnt2/β-catenin pathway inhibitors of the pyrido[2,3,-*b*]pyrazine core skeleton identified in the primary screening (the code name, DGG, was omitted before the numbers).

compounds toward Wnt/β-catenin pathway for new drug discovery area.[12]

Therefore, we have concentrated our attention on searching for novel small organic β-catenin inhibitors. We have previously found initial evidence showing that 2,3,4-trisubstituted quinoxaline derivatives are highly active β-catenin inhibitors that hold promise in lung cancer treatment.[13] In our previous report, that aimed to identify small molecule inhibitors of β-catenin, we first screened 1434 compounds[14,15] using a cell-based reporter assay that measures the transcriptional activity of β-catenin-TCF/LEF. It was dependent on Wnt signaling and could be used to monitor the activity of the Wnt signaling pathway.[16] The inhibition of cell proliferation of A549/Wnt2 cells by the 1434 compounds was screened at a compound concentration of 5 μM and compounds that reproducibly inhibited growth by over 50% were selected.[17] Thirteen number of 2,3,4-trisubstituted quinoxaline derivatives were shown reproducibly to have an IC_{50} below 5 μM. One of the best hit compound, **DGG-720**, exhibited the essential functional of a high activity due to the presence of the 3-ethynyl group. However, in our previous paper we could not find out good druggable lead compound via the introduction of 3-ethynyl series building blocks. Thus, based on our previous results, we have tested

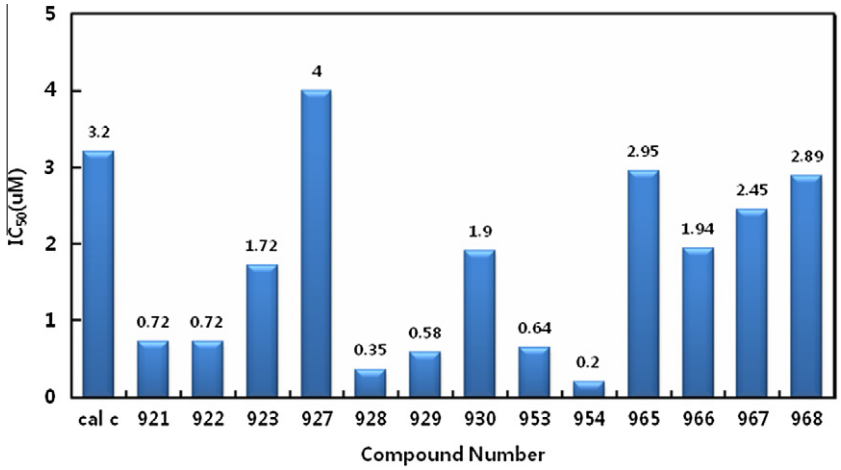

Figure 3. IC_{50} values of the 13 compounds selected from the 1st screening using the cytotoxicity assay with A549/Wnt2 cells. Cal C, calphostin C, the positive control.[20]

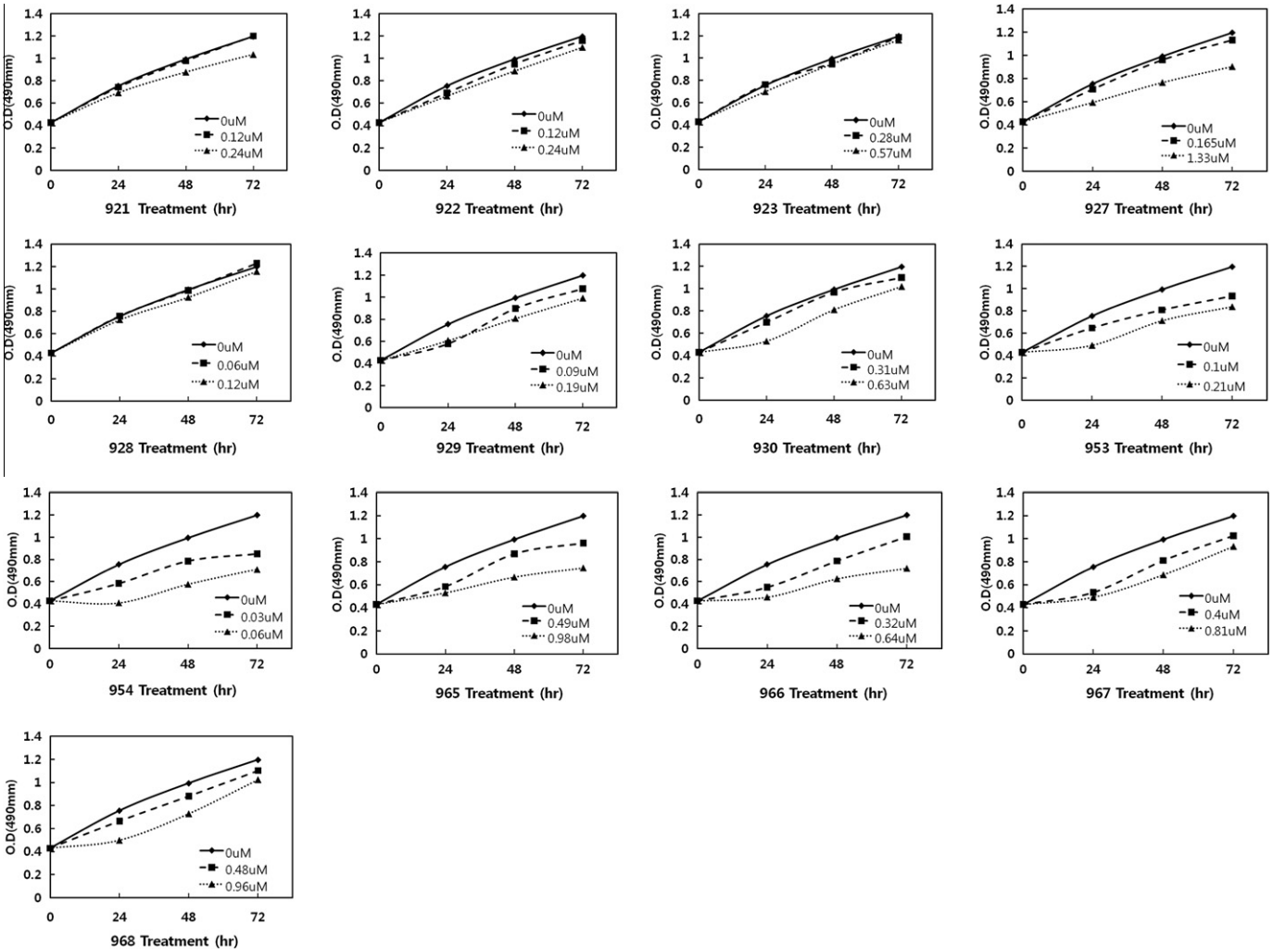

Figure 4. The effect of compounds chosen from the first screening on the cell proliferation at 15% and 30% of IC_{50} in A549/Wnt2 cells.

whether development of a new core skeleton based on the bioisostere concept compared with that of quinoxaline may improve the physicochemical properties as well as the cell proliferation of A549/Wnt2 cells.

2. Result and discussion

We designed a scaffold combining the quinoxaline moiety found in pyrido[2,3,-*b*]pyrazine with the pyridine ring system

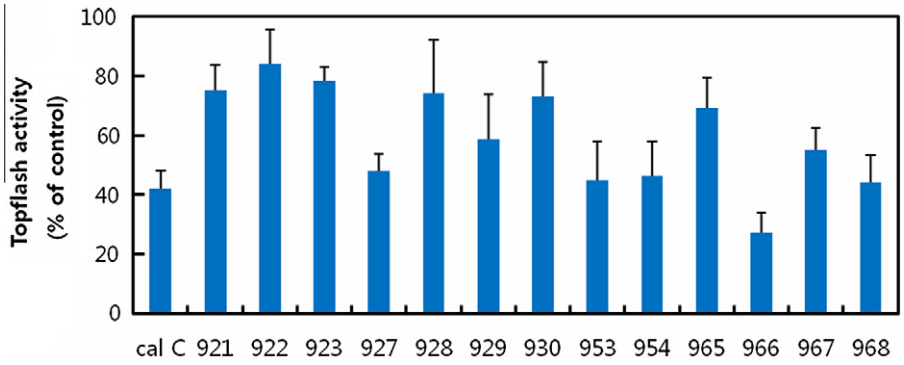

Figure 5. The effect of compounds chosen from the first screening on the TCF/β-catenin transcriptional activity at the IC_{50} of cell proliferation in A549 cells. Cal C, Calphostin C, the positive control.[20]

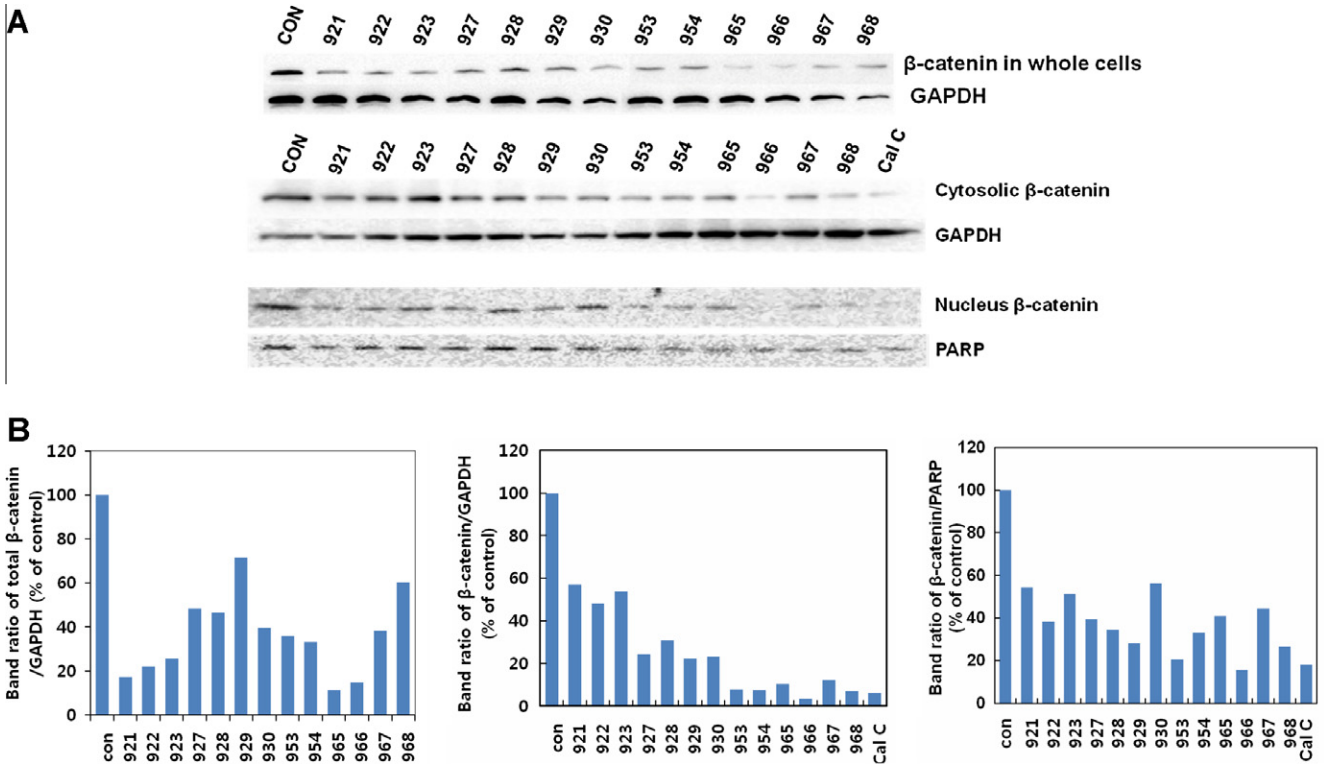

Figure 6. β-Catenin protein levels in total, cytosolic and nuclear fraction prepared from the A549/Wnt2 cells treated with the 13 first 'hit' compounds at the IC_{50} of cytotoxicity. (A) β-Catenin protein levels in total cell fraction, cytosol and nuclear fraction and (B) the band ratio of total β-catenin/GAPDH, cytosol β-catenin/GAPDH and nuclear β-catenin/PARP. GAPDH and PARP are reference proteins for the cytosolic and nuclear fractions, respectively.

(Fig. 1), and synthesized one hundred 3-arylethynyl-substituted pyrido[2,3,-*b*]pyrazine derivatives[16] designed via the bioisostere concept, as shown in Figure 1.[18] In the first round of screening, 13 pyrido[2,3,-*b*]pyrazine derivatives reproducibly exhibited an IC_{50} of cytotoxicity below 5 μM in A549/Wnt2 cells and were subjected to further screening,[19] as shown in Figures 2 and 3. In this study, we revealed that pyrido[2,3,-*b*]pyrazine structure (**DGG-954**) showed better physicochemical properties and stronger activity than quinoxaline (**DGG-720**). Especially, *A* log *P* (0.6) of the **954** compound having pyrido[2,3,-*b*]pyrazine structure showed much lower value than that of the quinoxaline core skeleton's **720** compound (1.29), as shown in Figure 1. We convinced this clue can make the possibility of much higher for developing new drug candidate.

To study the relationship between the cytotoxicity and the inhibition of cell proliferation, the effect of 13 selected compounds decreased cell proliferation about 15% and 30% of cytotoxicity IC_{50} values at 24 and 48 h, respectively using CellTiter 96 non-radioactive cell proliferation assay kit (Promega, USA) (Fig. 4). The differences of assays between cytotoxicity and cell proliferation were the cell seeding number and culture time as described in Section 4. Among 13 compounds, compounds **953, 954, 965** and **966** significantly inhibited the cell proliferation in a dose-dependent manner with 208, 43, 830, and 535 nM of IC_{50} values at 72 h, respectively. Their ratios of IC_{50} values in cell proliferation to cytotoxicity were 3.07–4.64.

Next, we examined the inhibitory effect of the 13 pyrido[2,3,-*b*] pyrazine hit compounds on the Wnt/β-catenin signal pathway at the cytotoxicity IC_{50} level determined in Figure 3. For the Topflash assay, A549/Wnt2 cells were transiently transfected with pSuper-Topflash with pRL/TK-which coded the renilla luciferase for the determination of the plasmid transfection efficiency- and treated

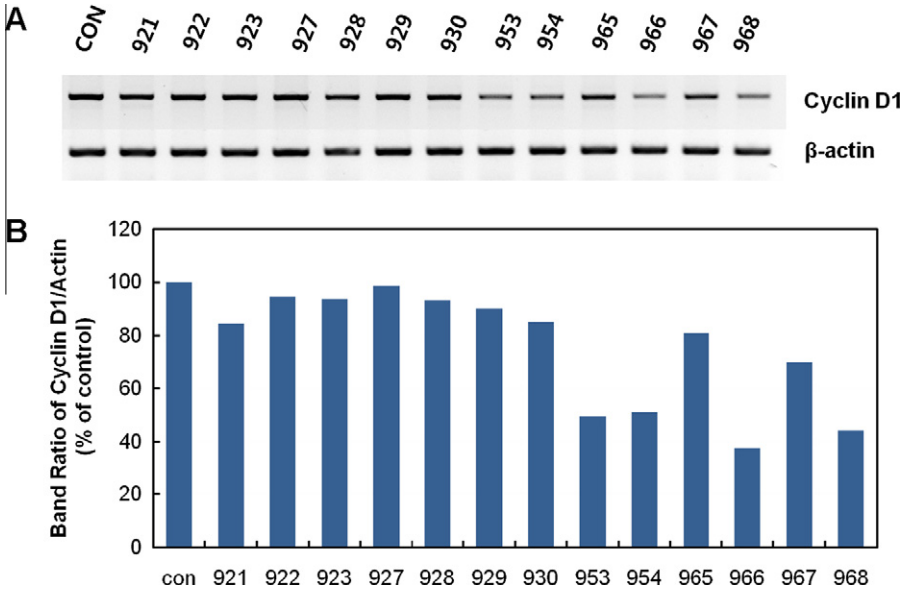

Figure 7. Effect of the 13 compounds on the mRNA expression of cyclin D1 in A549/Wnt2 cells: (A) RT-PCR band and (B) the band ratio of cyclin D1/Actin.

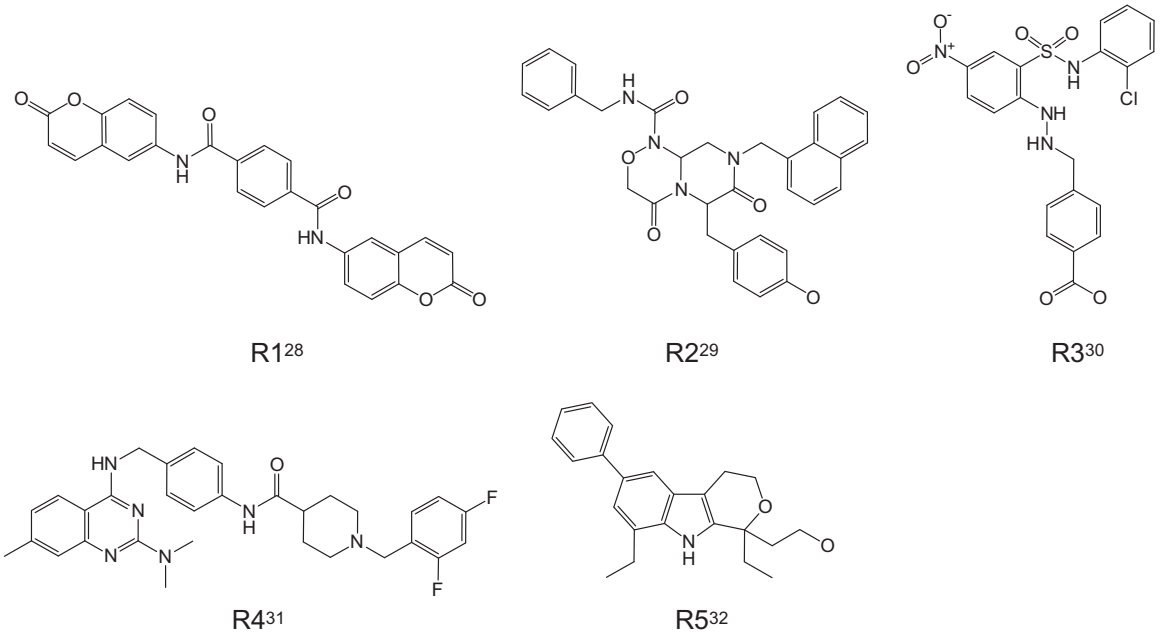

Figure 8. The reference compounds in the training set obtained from integrity.thomson-pharma.com site as Wnt inhibitors for building the pharmacophore model.

with the 13 compounds at IC_{50} (Fig. 5).[21] pFopflash, which has eight mutated TCF/LEF-binding sites and no response to the Wnt/β-catenin signal pathway, was used as the negative control. As shown in Figure 5, the 13 compounds inhibited the TCF/β-catenin reporter gene activity with a reduction of approximately 30–90% compared to the non-treated cells without significantly affecting the mutant reporter Fopflash. Compound **966** more strongly decreased the Topflash reporter activity to 30% compared to the cytotoxicity. Compounds **927**, **953**, **954** and **968** were similarly inhibited around 50% between the Topflash reporter gene activity and the cytotoxicity. Although the 13 compounds had structural similarity to the pyrido[2,3,-*b*]pyrazine core scaffold, the relationship between the inhibition rate of the Wnt/β-catenin signal pathway and the structure of the side chain could not be figured out.

The regulation of target genes in the Wnt/β-catenin pathway is dependent on the level of β-catenin and nuclear β-catenin is the hallmark of activated Wnt signaling. To compare the inhibition of the Wnt/β-catenin pathway with the change of β-catenin levels induced by these 13 compounds, their effect on the β-catenin protein level in cytosol and nuclear fractions was evaluated in A549/Wnt2 cells in using an immunoblot assay (Fig. 6).[22] These 13 compounds down-regulated the expression of the β-catenin protein all of three fractions, and compound **966** was the most effective inhibitor. Compounds **953**, **954** and **968** were decreased particularly in the nucleus β-catenin protein and these results accorded with the TopFlash assay. Collectively, our results suggested that the side chain structure with pyrido[2,3,-*b*]pyrazine core is important to determine the inhibition rate of the Wnt/β-catenin pathway.

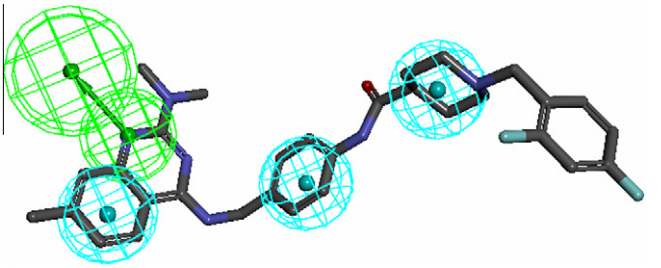

Figure 9. Pharmacophore mapping for reference compound **R4**, having fit value of 4.00. The green and cyan spheres represent the hydrogen-bond acceptor site and the hydrophobic sites, respectively.

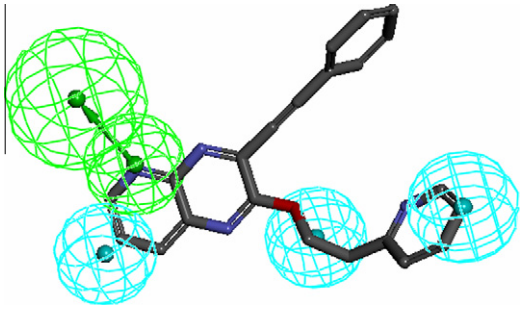

Figure 10. Pharmacophore mapping for compound **954**, having a fit value of 2.81.

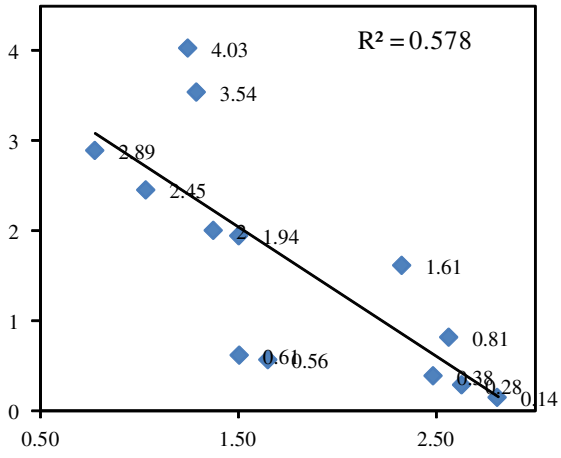

Figure 11. The correlation plot between pharmacophore mapping (fit values in *X*-axis) and activity (IC_{50} in *Y*-axis) for 13 hit compounds. Each dot is depicted as activity values.

Since the selected compounds inhibited the TCF/β-catenin transcriptional activity and cell proliferation, we further examined the expression of cyclin D1, which is related to cell progression and cell cycle progression and is a well-known Wnt/β-catenin signal target gene, in A549/Wnt2 cells. The gene expression level of cyclin D1 was inhibited by 24 h-treatment of compounds **953, 954, 966** and **968** (Fig. 7) and these results consistently agreed with results of Topflash assay (Fig. 5) and β-catenin levels in nucleus (Fig. 6).

We next studied a structure–activity relationship of pyrido[2,3,-*b*]pyrazine core skeleton hit compounds. To clearly investigate the structure–activity relationship studies of pyrido[2,3,-*b*]pyrazine core skeleton hit compounds, we selected 5 known compounds (R1–R5) from the Prous site (http://prous.integrity.com) as Wnt inhibitors and used them in the training set, as shown in Figure 8. After the 3D structures of these compounds were generated using CONCORD,[23] they were minimized using Gasteiger–Huckel charges and conjugated gradient methods. The common pharmacophores were generated using the HipHop algorithm.[24] Predefined pharmacophore features were used to automatically create the pharmacophore hypothesis model. The list of features of the minimum and maximum values was as follows: H-bond acceptor (Hba) 0 and 5, H-bond donor (Hbd) 0 and 5, Hydrophobic (Hy) 0 and 5. The compounds in the training set showed fit values ranging from 1.05 to 5.99. We have previously reported this model.[25]

Table 1
The fit values for 13 hit compounds shown in Figure 11

Inhibitor	Activity	Fit values
954	0.14	2.81
928	0.28	2.63
929	0.38	2.49
921	0.56	1.65
922	0.61	1.51
953	0.81	2.56
923	1.61	2.33
930	1.94	1.50
966	2.00	1.38
967	2.45	1.04
968	2.89	0.78
965	3.54	1.29
927	4.03	1.25

The pharmacophore mapping for reference compound **R4** having fit value of 4.0 is shown in Figure 9. The green and cyan spheres represent the hydrogen-bond acceptor site and the hydrophobic sites, respectively. The pharmacophore mapping for compound **954**, which presented the highest activity with a fit value of 2.81, is shown in Figure 10. The pharmacophore mapping for the compounds including **954** shown in Figure 10, pyrido[2,3,-*b*]pyrazine core had hydrogen-bond acceptor site and hydrophobic center roles. The distance for two hydrophobic sites in branch chains of pyrido[2,3,-*b*]pyrazine core is about 5.7 Å. The longer hydrophobic substituents have, better activity are obtained, such as **954**, **928** and **929**. And also, we could find out the correlation plot between pharmacophore mapping and activity for 13 hit compounds as shown in Figure 11 and Table 1.

3. Conclusion

In conclusion, we developed a novel 3-arylethynyl-substituted pyrido[2,3,-*b*]pyrazine as a first lead compound **954** by synthesizing one hundred pyrido[2,3,-*b*]pyrazine derivatives, of which 13 3-arylethynyl-substitutedpyrido[2,3,-*b*]pyrazine derivatives were identified as being able to inhibit the Wnt/β-catenin signal pathway and cell proliferation. And we have studied the pharmacophore mapping for compound **954**, which presented the highest activity with a fit value of 2.81. The pharmacophore mapping for the compounds including **954,** pyrido[2,3,-*b*]pyrazine core had hydrogen-bond acceptor site and hydrophobic center roles. Further studies are currently underway to optimize the potency and selectivity of these 13 derivatives and address their in vivo efficacy and therapeutic potential. These molecules may serve as useful mechanistic probes of the cellular function of the Wnt/β-catenin signal pathway and anticancer mechanism.

4. Experimental

4.1. Chemistry

4.1.1. General for synthesis

All chemicals were reagent grade and used as purchased. Reactions were monitored by thin layer chromatography (TLC) analysis using Merck Silica Gel 60 F-254 thin layer plates or attenuated

total reflection Fourier transform infrared (ATR-FTIR) analysis using TravelIR™ (SensIR Technology). Flash column chromatography was carried out on Merck Silica Gel 60 (230–400 mesh). The crude products were purified by parallel chromatography using Quad3™. ^{1}H NMR and ^{13}C NMR spectra were recorded in δ units relative to deuterated solvent as an internal reference using a Bruker 500 MHz NMR instrument. Liquid chromatography–mass spectrometry (LC–MS) analysis was performed on an electrospray ionization (ESI) mass spectrometer with photodiode-array detector (PDA) detection. LC–MS area percentage purities of all products were determined by LC peak area analysis (XTerraMS C_{18} column, 4.6 mm × 100 mm; PDA detector at 200–400 nm; gradient, 5–95% CH_3CN/H_2O). High-resolution mass spectrometry fast-atom bombardment (HRMS-FAB) spectra were obtained using API 4000Q TRAP LC/MS/MS system (Applied Biosystems).

4.2. Synthetic procedures for the preparation of 3-(phenylethynyl)-2-(2-(pyridin-2-yl)ethoxy)pyrido[3,2-*b*]pyrazine (Lead compound 954)

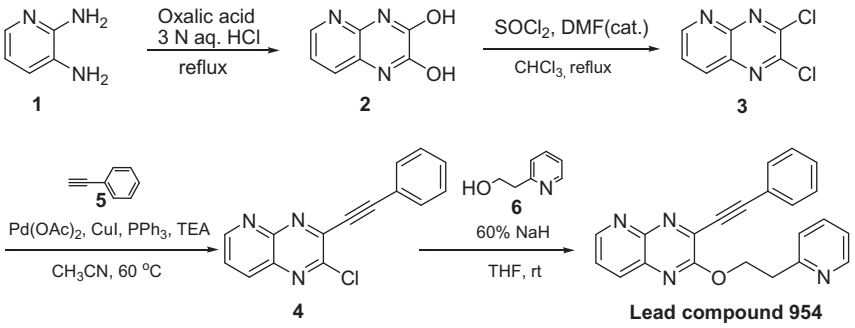

4.2.1. Synthesis of pyrido[3,2-*b*]pyrazine-2,3-diol (2)

A solution of pyridine-2,3-diamine (**1**) (5.0 g, 45.8 mmol) and oxalic acid (4.8 g, 53.3 mmol) in 3 N aq HCl (100 ml) was stirred at reflux condition for 24 h. The resulting mixture was filtered and then washed with cold water and dried in a vacuum oven at 50 °C. The desired product **2,** pyrido[3,2-*b*]pyrazine-2,3-diol, was obtained in good yield (89%, 6.7 g). ^{1}H NMR (500 MHz, DMSO) δ 7.13 (m, 1H), 7.46 (dd, J = 1.4, 6.3 Hz, 1H), 8.07 (m, 1H), 11.98 (s, 1H), 12.33 (s, 1H); MS (ESI) m/z 164 ([M+H]$^+$).

4.2.2. Synthesis of 2,3-dichloropyrido[3,2-*b*]pyrazine (3)

To a stirred solution of pyrido[3,2-*b*]pyrazine-2,3-dione (**2**) (4.2 g, 26.0 mmol) in chloroform ($CHCl_3$, 100 ml) was added thionyl chloride (9.3 g, 78.0 mmol) and *N*,*N*-dimethylformamide (DMF, 0.5 ml) at reflux condition for 24 h. The resulting mixture was concentrated in vacuo to remove the solvent and then water was added. The desired product was filtered and washed with water and dried in a vacuum oven at 50 °C. The desired product **3**, 2,3-dichloropyrido[3,2-*b*]pyrazine, was obtained in good yield (78%, 4.8 g). ^{1}H NMR (500 MHz, DMSO) δ 7.81 (m, 1H), 8.43 (dd, J = 6.6, 1.7 Hz, 1H), 9.19 (dd, J = 3.1, 1.5 Hz, 1H); MS (ESI) m/z 200 ([M+H]$^+$).

4.2.3. Synthesis of 2-chloro-3-(phenylethynyl)pyrido[3,2-*b*]pyrazine (4)

To a stirred solution of 2,3-dichloropyrido[3,2-*b*]pyrazine (**3**) (4.76 g, 18.5 mmol) in dimethylsulfoxide (DMSO, 2 ml) solution was added phenylacetylene (2.3 ml, 21.3 mmol), triethylamine (18.0 ml, 129.6 mmol), palladium(II) acetate (290 mg, 1.3 mmol), copper(I) iodide (437 mg, 1.7 mmol) and triphenylphosphine (388 mg, 2.0 mmol) at 80 °C for 2 h. The resulting mixture was concentrated in vacuum to remove the solvent and then water was added. The mixture was extracted with ethyl acetate and the organic layer was washed with water and dried over $MgSO_4$. After removal of solvent in vacuum, the residue was purified by SiO_2 column chromatography (CH_2Cl_2/*n*-hexane = 3:2) to yield the desired compound **4**, 2-chloro-3-(phenylethynyl)pyrido[3,2-*b*]pyrazine (83%, 4.6 g). ^{1}H NMR (500 MHz, $CDCl_3$) δ 7.46 (m, 6H), 7.73 (m, 6H), 8.34 (d, J = 8.3 Hz, 2H), 9.19 (dd, J = 2.31, 1.8 Hz, 2H); MS (ESI) m/z 266 ([M+H]$^+$).

4.2.4. Synthesis of 3-(phenylethynyl)-2-(2-(pyridin-2-yl)ethoxy) pyrido[3,2-*b*]pyrazine (Hit compound, 954)

To a stirred solution of 2-(pyridin-2-yl)ethanol (1.4 g, 11.6 mmol) in tetrahydrofuran (THF; 10 ml) solution was added sodium hydride dispersion (60%) in mineral oil (743 mg, 18.6 mmol) at room temperature for 20 min, after which THF (10 ml) solution of the prepared compound 4, 2-chloro-3-(phenylethynyl)pyrido[3,2-*b*]pyrazine (2.47 g, 9.3 mmol), was dropped for 1 h. Stirring was continued at room temperature for 8 h. The resulting mixture was concentrated in vacuo to remove the solvent and then water was added. The mixture was extracted with ethylacetate and the organic layer was washed with water and dried over $MgSO_4$. After removal of solvent in vacuo, the residue was purified by SiO_2 column chromatography (CH_2Cl_2/ethanol = 9:1) to yield the desired compound **954**, (79%, 2.84 g). ^{1}H NMR (500 MHz, $CDCl_3$) δ 3.42 (t, J = 6, 6.5 Hz, 2H), 4.96 (t, J = 6.5, 6.4 Hz, 2H), 7.13 (s, 1H), 7.37 (m, 4H), 7.55 (dd, J = 1.2, 4.2 Hz, 2H), 7.61 (t, J = 0.9, 7.1 Hz, 2H), 8.14 (d, J = 0.9 Hz, 1H), 8.51 (dd, J = 1.8, 6.5 Hz, 1H), 8.95 (dd, J = 1.1, 0.6 Hz, 1H); ^{13}C NMR δ 158.3, 157.0, 150.7, 149.6, 148.3, 136.4, 136.1, 135.7, 135.0, 132.6, 132.2, 132.1, 130.0, 128.6, 128.5, 125.2, 124.0, 121.8, 121.7, 97.6, 84.9, 77.4, 77.1, 76.9, 66.9, 37.6; MS (ESI) m/z 353 ([M+H]$^+$); HRMS-ESI (m/z): [M+H]$^+$ calcd for $C_{22}H_{16}N_4O_1$ 352.1324; found 353.143.

4.2.5. Synthesis of 3-(phenylethynyl)-2-(2-(pyrrolidin-1-yl)ethoxy)pyrido[3,2-*b*]pyrazine 921

^{1}H NMR (500 MHz, $CDCl_3$) δ 1.81 (s, 4H), 2.77 (s, 4H), 3.05 (t, J = 5.7 Hz, 2H), 4.72 (t, J = 5.7 Hz, 2H), 7.40–7.42 (m, 3H), 7.56 (t, J = 4.2 Hz, 1H), 7.65 (dd, J = 1.8, 6.3 Hz, 2H), 8.95 (dd, J = 1.8, 2.4 Hz, 1H); MS (ESI) m/z 345 ([M+H]$^+$).

4.2.6. Synthesis of 2-(1-methylpiperidin-3-yloxy)-3-(phenylethynyl)pyrido[3,2-*b*]pyrazine 922

^{1}H NMR (500 MHz, $CDCl_3$) δ 1.62 (d, J = 2.05 Hz, 1H), 1.72 (dd, J = 3.5, 7.0 Hz, 1H), 1.90 (m, 1H), 2.17 (t, J = 10.3 Hz, 2H), 2.31 (s, 3H), 2.35 (s, 1H), 2.64 (d, J = 11.21 Hz, 1H), 3.09 (d, J = 9.0 Hz, 1H), 5.36 (m, 1H) 7.39 (t. J = 4.9 Hz, 3H) 7.56 (dd, J = 4.2, 4.0 Hz,

1H), 7.63 (dd, *J* = 1.6, 6.0 Hz, 2H), 8.10 (dd, *J* = 1.8, 6.5 Hz, 1H), 8.88 (dd, *J* = 1.8, 2,4 Hz, 1H); MS (ESI) *m/z* 345 ($[M+H]^+$).

4.2.7. Synthesis of *N,N*-dimethyl-3-((3-(phenylethynyl)pyrido[3,2-*b*]pyrazin-2-yloxy)methyl) aniline 923

^{1}H NMR (500 MHz, $CDCl_3$) δ 2.96 (d, *J* = 5.74 Hz, 6H), 5.63 (s, 2H), 6.75 (s, 1H), 6.99 (d, *J* = 2.2 Hz, 2H), 7.40 (d, *J* = 1.52 Hz, 1H), 7.42 (d, *J* = 8.1 Hz, 3H), 7.59 (dd, *J* = 4.3, 4.0 Hz, 1H), 7.67 (dd, *J* = 1.5, 6.7 Hz, 2H), 8.19 (dd, *J* = 1.8, 6.4 Hz, 1H), 8.98 (dd, *J* = 1.8, 2.4 Hz, 1H); MS (ESI) *m/z* 381 ($[M+H]^+$).

4.2.8. Synthesis of 2-chloro-3-((3-methoxyphenyl)ethynyl)pyrido[3,2-*b*]pyrazine 927

^{1}H NMR (500 MHz, $CDCl_3$) δ 3.91 (t, *J* = 11.0, 8.4 Hz, 3H), 7.06 (m, 1H), 7.28 (d, *J* = 16.2 Hz, 1H), 7.37 (d, *J* = 7.5 Hz, 2H), 7.75 (dd, *J* = 4.2, 4.2 Hz, 1H), 8.39 (dd, *J* = 6.8, 1.5 Hz, 1H), 9.22 (dd, *J* = 1.8, 2,4 Hz, 1H); MS (ESI) *m/z* 296 ($[M+H]^+$).

4.2.9. Synthesis of 3-(3-((3-methoxyphenyl)ethynyl)pyrido[3,2-*b*]pyrazin-2-yloxy)-*N,N*-dimethylpropan-1-amine 928

^{1}H NMR (500 MHz, $CDCl_3$) δ 2.15 (m, 2H), 2.32 (d, *J* = 6.9 Hz, 6H), 2.62 (t, *J* = 7.3, 7.2 Hz, 2H), 3.84 (t, *J* = 7.5, 2.0 Hz, 3H), 4.63 (q, *J* = 6.7, 6.4, 6.4 Hz, 2H), 7.00 (s, 1H), 7.21 (dd, *J* = 1.2, 2.5 Hz, 1H), 7.29 (t, *J* = 5.4, 2.0 Hz, 1H), 7.32 (d, *J* = 7.9 Hz, 1H), 7.59 (dd, *J* = 4.3, 3.9 Hz, 1H), 8.15 (dd, *J* = 1.8, 6.5 Hz, 1H), 8.96 (dd, *J* = 1.8, 2.4 Hz, 1H); MS (ESI) *m/z* 363 ($[M+H]^+$).

4.2.10. Synthesis of 3-(3-((3,5-dimethoxyphenyl)ethynyl)pyrido[3,2-*b*]pyrazin-2-yloxy)-*N,N*-dimethylpropan-1-amine 929

^{1}H NMR (500 MHz, $CDCl_3$) δ 2.11 (m, 2H), 2.30 (s, 6H), 2.58(t, *J* = 7.3, 7.2 Hz, 2H), 3.81 (d, *J* = 11.1 Hz, 6H), 4.62 (t, *J* = 6.45, 6.45 Hz, 2H), 6.55 (t, *J* = 2.3, 2.2 Hz, 1H), 6.82 (d, *J* = 2.3 Hz, 2H), 7.57 (dd, *J* = 4.25, 4.0 Hz, 1H), 8.13 (dd, *J* = 1.7, 6.5 Hz, 1H), 8.95 (dd, *J* = 1.7, 2.5 Hz, 1H); MS (ESI) *m/z* 392($[M+H]^+$).

4.2.11. Synthesis of *N,N*-dimethyl-2-(3-(p-tolylethynyl)pyrido[3,2-*b*]pyrazin-2-yloxy) propan-1-amine 930

^{1}H NMR (500 MHz, $CDCl_3$) δ 1.49 (d, *J* = 6.3 Hz, 3H), 2.39 (s, 6H), 2.41 (s, 3H), 2.61 (dd, *J* = 4.5, 13.3 Hz, 1H), 2.79–2.83 (m, 1H), 7.22, (d, *J* = 7.9 Hz, 2H), 7.54–7.57 (m, 3H), 8.12 (dd, *J* = 1.8, 8.3 Hz, 1H), 8.93 (dd, *J* = 1.8, 4.2 Hz, 1H); MS (ESI) *m/z* 347 ($[M+H]^+$).

4.2.12. Synthesis of *N,N*-diethyl-2-(3-((4-methoxyphenyl)ethynyl)pyrido[2,3-*b*]pyrazin-2-loxy) ethan amine 953

^{1}H NMR (500 MHz, $CDCl_3$) δ 1.14 (t, *J* = 7.1 Hz, 6H), 2.78 (q, *J* = 7.2 Hz, 4H), 3.10 (t, *J* = 5.9 Hz, 2H), 3.86 (s, 3H), 4.68 (t, *J* = 5.9 Hz, 2H), 6.93 (dd, *J* = 1.9, 7.0 Hz, 2H), 7.57 (q, *J* = 4.3 Hz, 1H), 7.62 (dd, *J* = 1.9, 6.9 Hz, 2H), 8.14 (dd, *J* = 1.8, 8.3 Hz, 1H), 8.95 (dd, *J* = 1.8, 4.3 Hz, 1H); MS (ESI) *m/z* 377 ($[M+H]^+$).

4.2.13. Synthesis of 2-(3-((4-methoxy-2-methylphenyl)ethynyl)pyrido[3,2-*b*] pyrazin-2-yloxy)-*N,N*-dimethylethan amine 965

^{1}H NMR (500 MHz, $CDCl_3$) δ 2.41 (s, 6H), 2.62 (s, 3H), 2.89 (t, *J* = 5.8 Hz, 2H), 3.84 (s, 3H), 4.68 (t, *J* = 5.8 Hz, 2H), 6.76 (dd, *J* = 2.5, 8.5 Hz, 1H), 6.81 (d, *J* = 2.3 Hz, 1H), 7.54–7.56 (m, 1H), 7.58 (d, *J* = 8.6 Hz, 1H), 8.14 (dd, *J* = 1.6, 8.2 Hz, 1H), 8.93 (dd, *J* = 1.6, 4.2 Hz, 1H); MS (ESI) *m/z* 363 ($[M+H]^+$).

4.2.14. Synthesis of 2-(3-((3-fluorophenyl)ethynyl)pyrido[3,2-*b*] pyrazin-2-yloxy)-*N,N*-dimethyl ethan amine 966

^{1}H NMR (500 MHz, $CDCl_3$) δ 1.14 (t, *J* = 7.0 Hz, 6H), 2.76 (q, *J* = 7.0 Hz, 4H), 3.07 (t, *J* = 5.8 Hz, 2H), 4.69 (t, *J* = 5.8 Hz, 2H), 7.14 (t, *J* = 8.2 Hz, 1H), 7.36–7.38 (m, 2H), 7.44–7.46 (m, 1H), 7.60 (dd, *J* = 4.2, 8.2 Hz, 1H), 8.16 (dd, *J* = 1.6, 8.2 Hz, 1H), 8.97 (dd, *J* = 1.6, 4.2 Hz, 1H); MS (ESI) *m/z* 365 ($[M+H]^+$).

4.2.15. Synthesis of 3-((3-fluorophenyl)ethynyl)-2-(2-(pyrrolidin-1-yl)ethoxy) pyrido[3,2-*b*] pyrazine 967

^{1}H NMR (500 MHz, $CDCl_3$) δ 3.27 (s, 2H), 4.97 (s, 2H), 7.17 (s, 1H), 7.26 (s, 1H), 7.38 (t, *J* = 14.0, 5.7 Hz, 1H), 7.46 (d, *J* = 7.85 Hz, 1H), 7.59 (dd, *J* = 4.3, 3.8 Hz, 1H), 8.37 (dd, *J* = 6.6, 1.4 Hz, 1H), 8.99 (dd, *J* = 1.5, 2.5 Hz, 1H); MS (ESI) *m/z* 362($[M+H]^+$).

4.2.16. Synthesis of *N*-(2-(3-((3-fluorophenyl)ethynyl)pyrido[3,2-*b*]pyrazin-2-yloxy)thyl)-*N*-isopropylpropan-2-amine 968

^{1}H NMR (500 MHz, $CDCl_3$) δ 1.08 (d, *J* = 6.5 Hz, 12H), 2.95 (t, *J* = 6.9 Hz, 2H), 3.08–3.14 (m, 2H), 4.51 (t, *J* = 6.9 Hz, 2H), 7.15 (t, *J* = 8.3 Hz, 1H), 7.36–7.41 (m, 2H), 7.47 (d, *J* = 7.7 Hz, 1H), 7.59 (dd, *J* = 4.1, 8.3 Hz, 1H), 8.14 (dd, *J* = 1.7, 8.3 Hz, 1H), 8.96 (dd, *J* = 1.7, 4.1 Hz, 1H); MS (ESI) *m/z* 393 ($[M+H]^+$).

4.3. Biology

4.3.1. General for screening

4.3.1.1. Cell culture. The human lung carcinoma cell line A549 was obtained from American Tissue Type Culture Collection (Manassas, VA) and cultured in RPMI-1640 media supplemented with 10% fetal bovine serum (FBS, Gibco-BRL, USA), 100 U/ml penicillin G, and 100 U/ml streptomycin (Gibco-BRL, USA). Cell cultures were incubated at 37 °C in 5% CO_2/95% air, and the medium was replaced every third day.

4.3.1.2. Preparation of Wnt2 over-expressed cell line. A549/Wnt2 cells are over-expressed human Wnt2 by stable transfection of pUSEampWnt2, as described in Lee et al.[13] Briefly, A549 cells with 70% confluence in 60 mm culture were transfected with the pUSEampWnt2 or the empty vector using Transfast transfection reagent (Promega, USA). After 24 h of transfection, the medium was replaced with G418-containing medium which were selected for the stable transfectants.

4.3.1.3. Cytotoxicity and cell proliferation assay. Cells (8×10^3 for cytotoxicity or 3×10^3 cells/well for cell proliferation) were seeded onto 96-well microplates, allowed to attach for about 24 h and then treated with various concentrations of test compounds. After 24, 48 and 72 h, cell proliferation was determined by using a CellTiter 96 non-radioactive cell proliferation assay kit [MTS (3-(4,5-dimethylthiazol-2-yl)-5-(3-carboxymethoxyphenyl)-2-(4-sulfophenyl)-2*H*-tetrazolium) assay] according to the manufacturer's protocol (Promega, USA). For cytotoxicity test, cell viability was measured at 24 h after chemical treatment by MTS assay kit (Promega, USA). The plate was incubated at 37 °C in a CO_2 incubator for 30 min and the absorbance was measured on a Molecular Dynamic plate reader (Bio-Rad, Germany) at 490 nm.

4.3.1.4. Preparation of cytoplasmic, nuclear and whole cell extract. After the treatment of test chemicals for 24 h, cells were fractionated to cytoplasm and nuclear parts by the method of Wong.[20] Briefly, cells were washed two times with ice-cold phosphate-buffered saline (PBS) and resuspended in 400 ml of buffer A [10 mM HEPES at pH 7.9, 1.5 mM $MgCl_2$, 10 mM KCl, 0.5 mM DTT, 0.5 mM PMSF] supplemented with a complete protease inhibitor cocktail (Roche, USA). The cells were allowed to swell on ice for 15 min, lysed gently with 12.5 ml of 10% Nonide P-40, and centrifuged at 2000*g* for 10 min. The supernatant was collected and used as the cytoplasmic extracts. The nuclei pellet was resuspended in 40 ml of buffer C [20 mM HEPES, pH 7.9, 1.5 mM $MgCl_2$, 450 mM NaCl, 25% glycerol, 0.2 mM EDTA, 0.5 mM DTT, 0.5 mM PMSF] supplemented with a complete protease inhibitor cocktail (Roche, USA), incubated for 30 min in ice, and the nuclear debris was spun down at 20,000*g* for 15 min. The supernatant (nuclear extract) was collected, frozen in liquid nitrogen and stored at −80 °C until ready

for analysis. The protein content was determined using the Bradford Assay (Bio-Rad, Germany).

4.3.1.5. Western blot analysis. Protein samples (20–30 μg of protein) were subjected to sodium dodecyl sulfate–polyacrylamide gel electrophoresis (SDS–PAGE) and transferred to nitrile cellulose membranes (Whatman, Germany) for Western blotting. The primary antibodies used were β-catenin, GAPDH and PARP (Santa Cruz Biotechnology, Santa Cruz, USA). Immunoreactive proteins were visualized with enhanced chemiluminescence (ECL; Amersham Biosciences, USA) according to the manufacturer's protocol.

4.3.1.6. Transfection and luciferase reporter gene assay. Cells were transfected with the luciferase reporter constructs pSuper-Topflash containing eight TCF consensus binding sites upstream of firefly luciferase cDNA, or pSuperFopflash, a plasmid with mutated TCF binding sites (kindly provided by professor Ja-Hyun Baek at the School of Life Sciences and Biotechnology at Korea University, Seoul, Korea). Cells were transfected using Lipofectamine 2000 (Invitrogen Co., USA) with reporter construct and pRL-TK plasmid and incubated with various concentrations of the selected compounds at 37 °C. After 24 h, cells were lysed in 50 μl passive lysis buffer (Promega, USA). Firefly luciferase and renilla luciferase activity were determined by using the Dual-Glo Luciferase Assay System (Promega, USA). Results are expressed as the mean ± SEM of normalized ratios of firefly luciferase activity and renilla luciferase activity measurements for each triplicate set.

Acknowledgments

This research was supported by grants from the National R&D Program for Cancer Control (grant number 1020050), and from the Seoul Research and Business Development Program (grant number 10574), and the National Research Foundation of Korea (2010-0004128) funded by the Ministry of Education, Science and Technology, and by the Ministry of Knowledge Economy, Korea.

Supplementary data

Supplementary data associated with this article can be found, in the online version, at doi:10.1016/j.bmc.2011.07.028.

References and notes

1. Moon, R. T.; Brown, J. D.; Torres, M. *Trends Genet.* **1997**, *13*, 157.
2. Nusse, R. *Trends Genet.* **1999**, *15*, 1.
3. Chesire, D. R.; Ewing, C. M.; Sauvageot, J.; Bova, G. S.; Isaacs, W. B. *Prostate* **2000**, *45*, 323.
4. Morin, P. J.; Sparks, A. B.; Korinek, V.; Barker, N.; Clevers, H.; Vogelstein, B.; Kinzler, K. W. *Science* **1997**, *275*, 1787.
5. Van Scoyk, M.; Randall, J.; Sergew, A.; Williams, L. M.; Tennis, M.; Winn, R. A. *Transl. Res.* **2008**, *151*, 175.
6. Katoh, M. *Int. J. Oncol.* **2001**, *19*, 1003.
7. Park, J. K.; Song, J. H.; He, T. C.; Nam, S. W.; Lee, J. Y.; Park, W. S. *Neoplasma* **2009**, *56*, 119.
8. Cheng, X. X.; Wang, Z. C.; Chen, X. Y.; Sun, Y.; Kong, Q. Y.; Liu, J.; Li, H. *Cancer Lett.* **2005**, *223*, 339.
9. Watanabe, O.; Imamura, H.; Shimizu, T.; Kinoshita, J.; Okabe, T.; Hirano, A.; Yoshimatsu, K.; Konno, S.; Aiba, M.; Ogawa, K. *Anticancer Res.* **2004**, *24*, 3851.
10. You, L.; He, B.; Xu, Z.; Uematsu, K.; Mazieres, J.; Mikami, I.; Reguart, N.; Moody, T. W.; Kitajewski, J.; McCormick, F.; Jablons, D. M. *Oncogene* **2004**, *23*, 6170.
11. (a) Barker, N.; Clevers, H. *Nat. Rev. Drug Disc.* **2006**, *5*, 997; (b) McMillan, M.; Kahn, M. *Drug Discovery Today* **2005**, *10*, 1467.
12. (a) Saraswati, S.; Alfaro, M. P.; Thorn, C. A.; Atkinson, J.; Lee, E.; Young, P. P. *PLoS One* **2010**, *5*, e15521; (b) Lu, J.; Ma, Z.; Hsieh, J.-C.; Fan, C.-W.; Chen, B.; Longgood, J. C.; Williams, N. S.; Amatruda, J. F.; Lum, L.; Chen, C. *Bioorg. Med. Chem. Lett.* **2009**, *19*, 3825; (c) William, J. M.; Jeffrey, C. K.; Ramesh, B.; Peter, V. N. B.; Fukuyama, S.; Krishnamurthy, G.; Ronald, L. M.; Keith, P.; Barb, S.; Eugene, J. T. *Bioorg. Med. Chem.* **2010**, *18*, 190; (d) Kouken, K.; Midori, A. A.; Li, X.; Masami, I. *Bioorg. Med. Chem. Lett.* **2007**, *15*, 4254; (e) Wang, H.; Hao, J.; Hong, C. *Chem. Biol.* **2011**, *6*, 192.
13. Lee, S.-B.; Park, Y. I.; Dong, M. S.; Gong, Y.-D. *Bioorg. Med. Chem. Lett.* **2010**, *20*, 5900.
14. We have synthesized various drug-like heterocyclic libraries[15] more than 20,000 small molecules by combinatorial synthetic technology. In the first stage, we selected 1434 representative compounds by virtual screening based on drug-like property considering with known Wnt pathway inhibiters.
15. (a) Gong, Y.-D.; Lee, T. *J. Comb. Chem.* **2010**, *12*, 393; (b) Hwang, J. Y.; Choi, H.-S.; Seo, J.-S.; La, H.-J.; Yoo, S.-E.; Gong, Y. D. *J. Comb. Chem.* **2006**, *8*, 897; (c) Hwang, J. Y.; Gong, Y. D. *J. Comb. Chem.* **2006**, *8*, 297; (d) Hwang, J. Y.; Choi, H. S.; Lee, D. H.; Yoo, S. E.; Gong, Y. D. *J. Comb. Chem.* **2005**, *7*, 136; (e) Hwang, J. Y.; Choi, H. S.; Lee, D. H.; Gong, Y. D. *J. Comb. Chem.* **2005**, *7*, 816; (f) Lee, I. Y.; Kim, S. Y.; Lee, J. Y.; Yu, C.-M.; Lee, D. H.; Gong, Y. D. *Tetrahedron Lett.* **2004**, *45*, 9319.
16. (a) Gong, Y.-D.; Jeon, M. K.; Hwang, S. H.; Dong, M. S.; Lee, S. B.; Kang, K. H.; Oh, C. H. Novel 2-Sustituted Aminoalkylenyloxy-3-Substituted Phenyl Ethynyl Quinoxaline Derivatives, Korea Pat. No. 0889389.; (b) Gong, Y.-D.; Dong, M. S.; Hwang, S. H.; Lee, T. I.; Lee, S. B. 2-Sustituted Aminoalkylenyloxy-3-Substituted Phenylethynyl-6-Amino Quinoxaline, Korea Pat. Appl. No. 2008-0076221.
17. *Cell proliferation assay*: Cell proliferation was determined by using a CellTiter 96 non-radioactive cell proliferation assay kit according to the manufacturer's protocol (Promega, USA). The detail procedure was mentioned in biological experimental part.
18. Lee, S. J.; Gong, Y.-D.; Jeon, M. K.; Moon, S. H.; Jun, K. H.; Kim, J. M.; Lee, S. H.; Lee, H. H.; Kang, M. J. 2-Arylalkylenyloxy-3-Ethynylpyrido[2,3-*b*] Pyrazine Derivatives, Korea Pat. App. No. 2006-0063214.
19. We checked cytotoxicity of the 13 compounds in human lung fibroblast cell line (LL47) and were over 0.5–1.0 μM higher than those in A549 cells.
20. In the early stage of our research, we used Calphostin C as positive control since we could not obtain other known comparison inhibitors from commercial market. And then we have synthesized and used the Pfizer lead compound (Data Monitor Research Store: preclinical stage, pyrinium pamoate) as positive control.
21. Wong, B. C. Y.; Jiang, X. H.; Fan, X. M.; Lin, M. C. M.; Jiang, S. H.; Lam, S. K.; Kung, H. F. *Oncogene* **2003**, *22*, 1189.
22. Chalet, T.; Rita, G. N.; Anthony, J. R.; Beata, P.; Fatima, K.; Zhaobin, Z.; Huanchun, Z.; Quincy, T.; Ainsley, C. N.; Paraskevi, G.; Wei, Z.; Jeffrey, J. O.; Manuela, M. P.; Nicolaou, K. C.; Erwin, G. V. M. *Cancer Res.* **2005**, *65*, 605.
23. Concord; Tripos Inc., 1699 South Hanley Road, St. Louis, MO 63144.
24. Catalyst User Guide, Accelrys Software Inc., San Diego, 2005.
25. Gong, Y.-D.; Kang, N. S. *Bull. Korean Chem. Soc.* **2010**, *31*, 2039.